Nanotechnology **20** (2009) 095203 (7pp) doi:10.1088/0957-4484/20/9/095203

The effect of excimer laser annealing on ZnO nanowires and their field effect transistors

Jongsun Maeng, Sungho Heo[1], Gunho Jo, Minhyeok Choe, Seonghyun Kim, Hyunsang Hwang and Takhee Lee[2]

Department of Materials Science and Engineering, Gwangju Institute of Science and Technology, Gwangju 500-712, Korea

E-mail: tlee@gist.ac.kr

Received 15 October 2008, in final form 2 January 2009
Published 6 February 2009
Online at stacks.iop.org/Nano/20/095203

Abstract

We have investigated the effect of excimer laser annealing on the chemical bonding, electrical, and optical properties of ZnO nanowires. We demonstrate that after laser annealing on the ZnO nanowire field effect transistors, the on-current increases and the threshold voltage shifts in the negative gate bias direction. These electrical results are attributed to the increase of oxygen vacancies as n-type dopants after laser annealing, consistent with the shifts towards higher binding energies of Zn 2p and O 1s in the x-ray photoelectron spectroscopy analysis of as-grown nanowires and laser-annealed ZnO nanowires.

(Some figures in this article are in colour only in the electronic version)

1. Introduction

One-dimensional systems, such as nanowires and nanotubes, have attracted interest due to their potential applications as building blocks for nanoscale transistors, sensors, and optoelectronic devices [1–4]. ZnO nanowires especially have received considerable attention due to their unique properties, such as a wide direct bandgap (∼3.37 eV), a large exciton binding energy (∼60 meV), and piezoelectricity [3–7]. As a post-fabrication process, thermal annealing or laser annealing has been employed in order to improve the electrical properties of ZnO materials [8, 9]. In particular, laser annealing is a useful method because the nanosecond pulse duration of an excimer laser can induce low thermal budget processing and heating confinement near the surface region [10, 11]. For example, Aoki *et al* studied ZnO p–n diode fabrication by phosphorous doping as p-type dopants, using the KrF excimer laser annealing of an Zn_3P_2 film on a single n-type ZnO wafer [12]. Oh *et al* reported a high quality Pt Schottky contact to an n-type ZnO wafer, improving the electrical conductivity of the n-type ZnO wafer after KrF excimer laser annealing [9]. In addition, the effects of KrF excimer laser annealing on the optical and structural properties of ZnO films have also been studied [13–15]. However, compared with the many studies about the laser annealing on ZnO bulk and films, little research has been done on the effects of laser annealing on ZnO nanowires.

In this study, we investigated the effects of excimer laser annealing on ZnO nanowires and their field effect transistors (FETs). The structural, chemical bonding, optical, and electrical properties of ZnO nanowires and FET devices before and after laser annealing were studied. With recrystallization on the ZnO nanowire surface by excimer laser annealing, the capability of generating oxygen vacancies as n-type dopants is demonstrated.

2. Experimental details

The ZnO nanowires in this study were synthesized by the vapour–liquid–solid (VLS) mechanism using a carbothermal reduction process with hot-wall chemical vapour deposition. A c-plane sapphire substrate was coated with a ∼2 nm thick gold film using an electron-beam evaporator. The gold film on the substrate was transformed into molten nanoparticles during the process of heating, and these nanoparticles served as catalysts for nanowire growth in the VLS mechanism. The mixed sources of ZnO and graphite (4:1 ratio) and the substrate

[1] Present address: Samsung electronics, Nongseo-dong, Giheung-gu, Yongin, Gyeonggi-do 449-711, Korea.
[2] Author to whom any correspondence should be addressed.

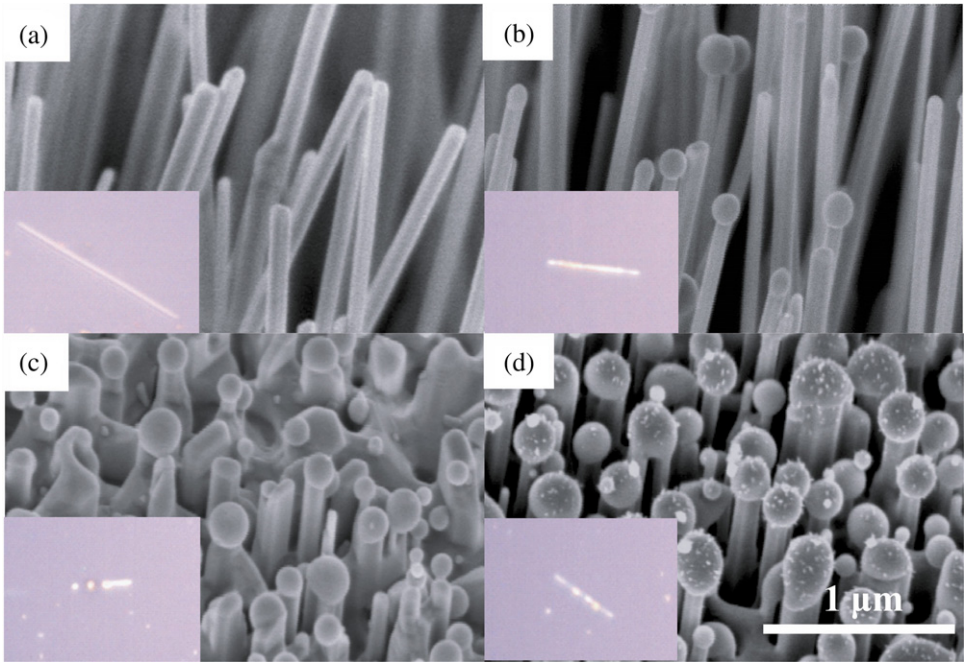

Figure 1. (a) FESEM image of as-grown ZnO nanowires on Au-coated sapphire substrate. ((b)–(d)) FESEM images of laser-annealed ZnO nanowires at fluences of 50, 100, and 200 mJ cm^{-2}, respectively.

on the alumina boat were inserted into the tube furnace. The tube was sealed and pumped with a mechanical pump. The mixture gas of N_2 (99%)/O_2 (1%), which serves as the source of elemental oxygen for nanowire growth, was supplied at a flow rate of 100 sccm, and the tube was filled with this gas at 700 Torr. Then, the temperature was increased to 920 °C and held for 20–30 min during the nanowire growth. The grown ZnO nanowires were examined with a field emission scanning electron microscope (FESEM, HITACHI S-4700) and a high resolution transmission electron microscope (HRTEM, Tecnai F20).

The excimer laser annealing was performed in a chamber filled with a N_2 (97%)/H_2 (3%) mixture gas at a pressure of 100 Torr with a KrF excimer laser. The excimer laser in our experiment is a homogenized KrF laser with an ultraviolet wavelength (248 nm) and a short pulse time (25 ns). The fluence of the excimer laser used in our study was 50, 100, 200, and 300 mJ cm^{-2}, as measured by a power meter. Due to the high laser energy density and short pulse, the ZnO surface first melts and then cools down rapidly [8]. Therefore, the excimer laser annealing is expected to be an effective structural and electrical tuning method for ZnO nanowires due to the laser irradiation with a short pulse time on the small dimension ZnO nanomaterials.

The effects of the laser annealing on the structural, chemical bonding, optical, and electrical properties of ZnO nanowires were investigated with FESEM, HRTEM, photoluminescence (PL) spectra, x-ray photoelectron spectroscopy (XPS), and current–voltage (I–V) characterizations, respectively. In particular, the ZnO nanowires were fabricated into FET device structures to study the influence of laser annealing on their electrical properties (see figures 5(a) and (b)). To fabricate ZnO nanowire FET devices, individual ZnO nanowires suspended in isopropyl alcohol were dropped onto a 100 nm thick thermally-grown oxide on silicon. The silicon substrate was a highly-doped p-type substrate that could serve as a back gate. Metal electrodes consisting of Ti (50 nm)/Au (50 nm) were then deposited by an electron-beam evaporator and defined as the source and drain electrodes by photolithography and a lift-off process. The source and drain electrodes were typically separated by ∼3 μm. The electrical properties, such as drain–source current versus voltage characteristics as a function of drain voltage and gate voltage, were measured using a semiconductor parameter analyser (Agilent B-1500). The measured electrical properties of ZnO nanowire FETs were compared before and after laser annealing.

3. Results and discussion

3.1. Surface morphology and structural properties

Figure 1(a) shows an FESEM image of ZnO nanowires on the growth substrate before laser annealing, and figures 1(b)–(d) are FESEM images of ZnO nanowires on the growth substrates after laser annealing at fluences of 50, 100, and 200 mJ cm^{-2}, respectively. As the fluence increased, the vertically-grown ZnO nanowires began to melt from the top of the nanowires. This is because the photon energy of the KrF excimer laser used in our experiments (479.6 kJ mol^{-1}) is enough to break Zn–O bonds (248 kJ mol^{-1}) [9, 13]. The insets of figure 1 show optical images of ZnO nanowires transferred onto Si substrates from the growth substrates without laser annealing (figure 1(a) inset) and followed by laser annealing at the same fluences of 50, 100, and 200 mJ cm^{-2} (insets of figures 1(b)–(d)). At a high fluence such as 100 and 200 mJ cm^{-2}, the ZnO nanowires started to melt and broke into pieces. It has been reported that laser annealing with a high fluence

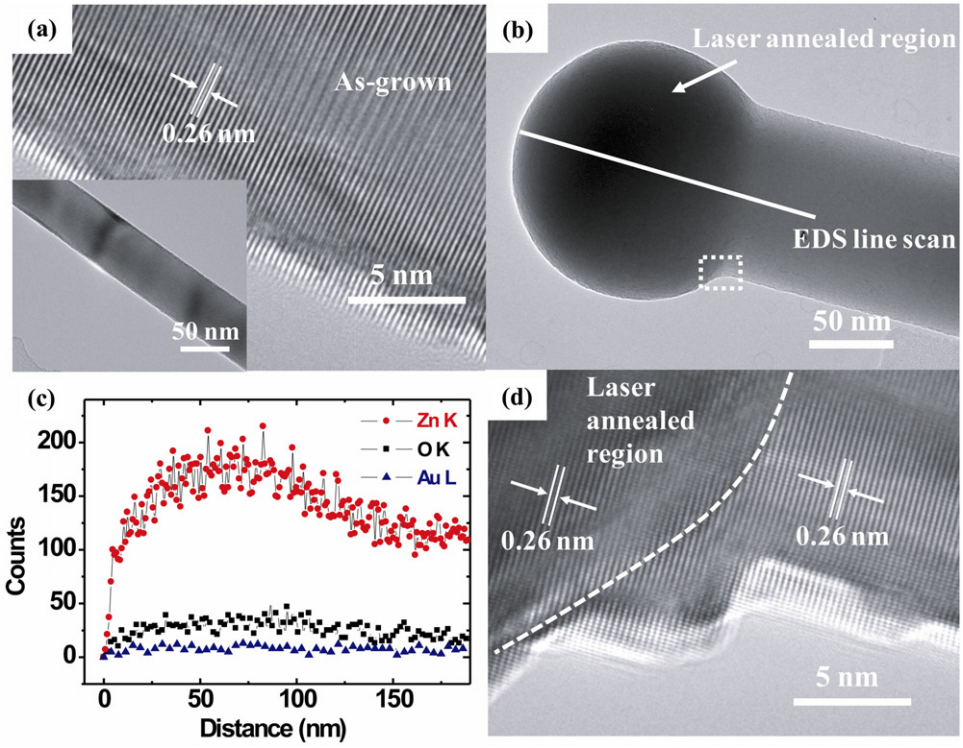

Figure 2. (a) HRTEM image of an as-grown ZnO nanowire. The inset is a low magnification TEM image showing a smooth and straight ZnO nanowire. (b) TEM image of a laser-annealed ZnO nanowire at a fluence of 50 mJ cm^{-2}. (c) EDX data obtained from the line scan indicated in (b). (d) HRTEM image obtained for the area marked in (b).

($\geqslant$150 mJ cm^{-2}) can even transform the amorphous phase into the crystalline phase of ZnO films [14].

Figure 2 shows HRTEM images of as-grown ZnO nanowires and ZnO nanowires detached from the growth substrate after laser annealing at a fluence of 50 mJ cm^{-2}. Figure 2(a) shows an HRTEM image of as-grown ZnO nanowires before laser annealing. The average atomic spacing along the growth direction was ∼0.26 nm, and the lattice spacing of the (0001) planes of wurtzite ZnO corresponds to ∼0.52 nm [16, 17]. The low resolution TEM image (inset of figure 2(a)) indicates the straight and smooth surface of an as-grown ZnO nanowire with a uniform diameter along the nanowire. Figure 2(b) is a TEM image of a ZnO nanowire detached from the growth substrate after laser annealing, and it shows that the end of the nanowire has changed into a spherical tip shape. Energy dispersive x-ray (EDX) analysis from a line scan on the ZnO nanowire in figure 2(b) is displayed in figure 2(c). The EDX results indicate that there is an excess of Zn in the spherical tip region of the ZnO nanowire relative to the other nanowire region that was not influenced by laser annealing. The oxygen vapour pressure is much higher than the vapour pressure of zinc in ZnO [18, 19], and the ZnO results in a stoichiometric excess of Zn [19]. Therefore, it is expected that the surface melting of ZnO nanowires by laser annealing in a vacuum chamber that lacks oxygen induces Zn-rich ZnO nanowires due to increased oxygen vacancies [20]. Figure 2(d) shows lattice images near the boundary of the spherical tip region (laser-annealed region) and the nanowire region that was not influenced by laser annealing. The atomic spacing of the ZnO nanowire in both regions was identical as ∼0.26 nm. This result suggests that single crystals of ZnO nanowires were kept from melting and recrystallization by laser annealing at 50 mJ cm^{-2}.

3.2. Optical properties

In order to investigate the optical properties of ZnO nanowires, PL measurements were carried out in the range of 2.2 and 3.5 eV. Deep level luminescence such as the green band was not obviously observed before and after laser annealing, as shown in figure 3. Figure 3 shows PL spectra obtained at room temperature for as-grown nanowires and laser-annealed nanowires with fluences of 50, 100, 200, and 300 mJ cm^{-2}. Both the as-grown nanowires and laser-annealed nanowires showed near-band emission (ultraviolet (UV) emission) at ∼3.26 eV, which is attributed to free exciton emission and its first longitudinal optical phonon replicas of free exciton [21, 22].

The intensity of the UV emission peaks was reduced after laser annealing, except in the case of laser annealing with a fluence of 50 mJ cm^{-2}. The PL intensity is closely related to the crystallinity and roughness of ZnO materials. For example, Aoki *et al* reported that the decrease in the UV emission intensity resulted from a deterioration of the surface crystallinity of single crystal ZnO wafers due to laser annealing with a high fluence such as 150 mJ cm^{-2} [12]. On the other hand, Zhao *et al* observed that polycrystalline ZnO thin films showed more intense UV emission after laser annealing, as compared with as-grown ZnO thin films [13]. They reported that an optimum fluence of ∼450 mJ cm^{-2} could lead to the

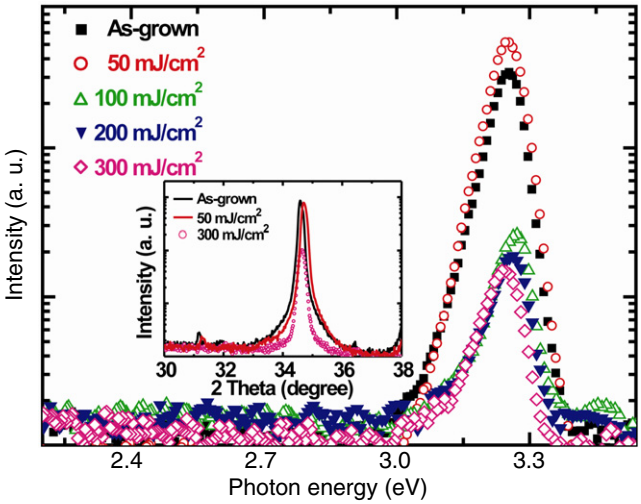

Figure 3. PL spectra of as-grown nanowires and laser-annealed nanowires at the fluences of 50, 100, 200, and 300 mJ cm^{-2}. The inset shows XRD patterns in the (0002) plane of the as-grown and laser-annealed ZnO nanowires at the fluences of 50 and 300 mJ cm^{-2}.

most intense UV emission after laser annealing and a higher fluence of 650 mJ cm^{-2} showed lower photoluminescence intensity accompanied with increased surface roughness and decreased crystallinity while maintaining a good epitaxial orientation and the wurtzite crystal structure of the ZnO film [13].

The trend of the change in UV emission intensity in figure 3 is due to the results that the ZnO nanowires after laser annealing at 50 mJ cm^{-2} maintained nanowire morphology, whereas the morphology and crystallinity of ZnO nanowires after laser annealing at higher energies changed considerably. The inset of figure 3 shows x-ray diffraction (XRD) patterns (theta–2 theta scan) of the as-grown and laser-annealed ZnO nanowires at the fluences of 50 and 300 mJ cm^{-2}. The XRD pattern of as-grown ZnO nanowires was measured at 34.5° of the intense (0002) plane peak, which indicates single phase with the preferred (0002) orientation. The (0002) diffraction intensity of the laser-annealed ZnO nanowires at the fluence of 50 mJ cm^{-2} was comparable with that of as-grown nanowires. However, the (0002) diffraction intensity of the laser-annealed ZnO nanowires at the fluence of 300 mJ cm^{-2} significantly decreased, which implies a poor crystallinity of ZnO nanowires. Laser annealing at a high fluence above 50 mJ cm^{-2} caused deterioration in the morphology and crystallinity of ZnO nanowires. The ZnO nanowires even broke into pieces at higher fluences (see figure 1). Therefore, the ZnO nanowires at 50 mJ cm^{-2} exhibited similar UV emission as the as-grown nanowires, but the UV emission decreased for the laser-annealed ZnO nanowires at energies above 50 mJ cm^{-2}.

3.3. Chemical bonding by XPS analysis

XPS analysis was performed to study the chemical bonding of ZnO nanowires before and after laser annealing. We expected that the chemical bonding of ZnO nanowires could influence the electrical properties of ZnO nanowires, mainly due to an increase of oxygen vacancies that act as n-type dopants. The XPS measurements shown in figure 4 were performed for three sets of nanowires: as-grown nanowires and laser-annealed nanowires at 50 and 200 mJ cm^{-2}. The binding energies of O 1s and Zn 2p were calibrated by taking the binding energy of the C 1s peak (285.0 eV) as the reference in XPS. As compared with the as-grown nanowires, the laser-annealed nanowires show the peak of the Zn 2p spectrum shifted towards a higher binding energy by 0.1–0.7 eV, which is ascribed to the zinc enrichment by recrystallization caused by laser annealing [6]. Figure 4(b) shows that the O 1s peak has shoulders at higher binding energies. For the laser-annealed nanowires at 200 mJ cm^{-2}, the O 1s peak is decomposed into three peaks. Among these three peaks, the dominant one is located at 530.9 eV (O1), which is assigned to the O^{2-} ion in the wurtzite structure surrounded by the Zn atoms with their full complement of nearest-neighbour O^{2-} ions [23]. The peak located at 532.5 eV (O2) is assigned to the O^{2-} ion in the zinc oxyhydroxide species, ZnO(OH), and the peak at 533.5 eV (O3) is ascribed to loosely bound oxygen, such as absorbed O^2 or adsorbed H_2O on the ZnO surface [8, 23, 24].

The peak of O 1s also shifted towards higher binding energies as the fluence was increased. For example, for the case

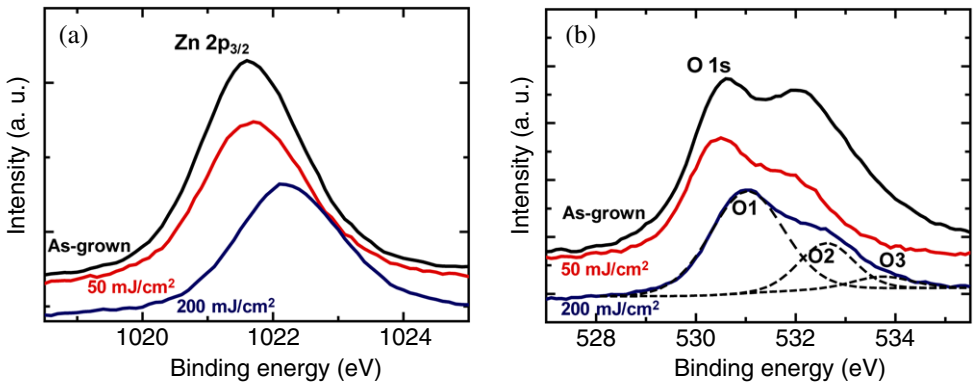

Figure 4. XPS spectra obtained from as-grown nanowires and laser-annealed nanowires with fluences of 50 and 200 mJ cm^{-2}. (a) Zn $2p_{3/2}$ spectra. (b) O 1s spectra.

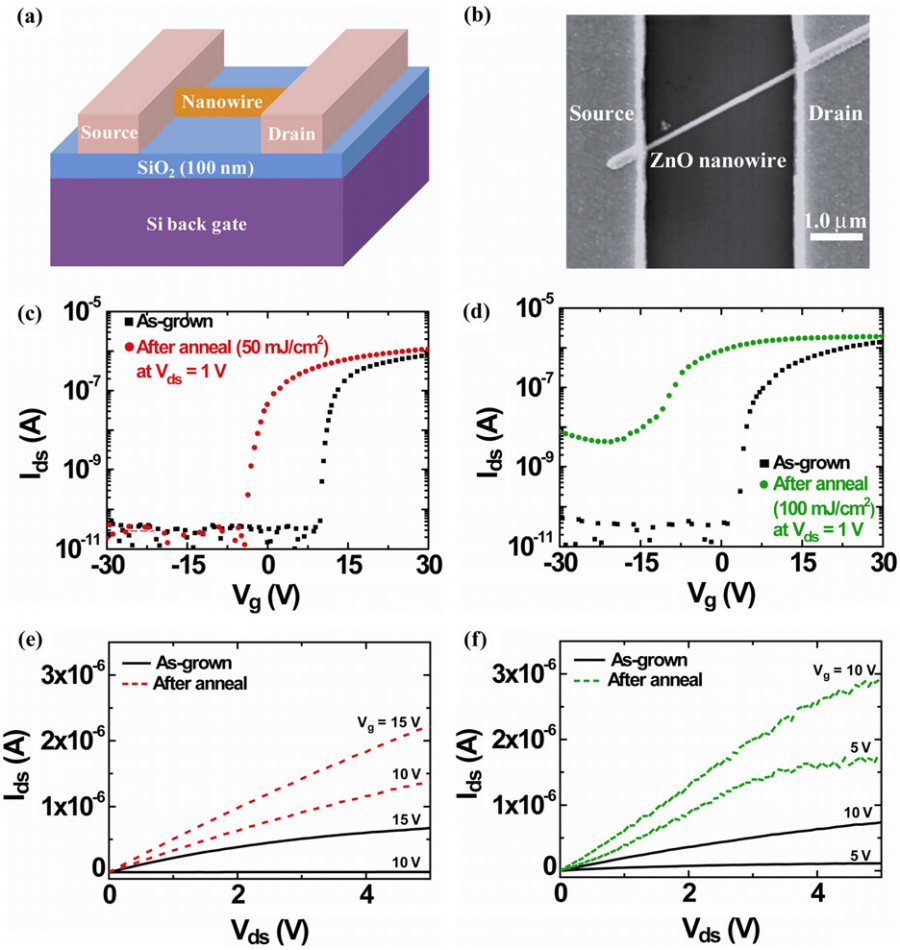

Figure 5. (a) Schematic diagram of a ZnO nanowire FET. (b) FESEM image of a ZnO nanowire across metal electrodes. The I_{ds}–V_g curves ((c) and (d)) measured at $V_{ds} = 1.0$ V and I_{ds}–V_{ds} curves ((e) and (f)) at different gate voltages with a step of 5 V for ZnO nanowire FETs. ((c) and (e)) Before and after laser annealing at a fluence of 50 mJ cm^{-2}. ((d) and (f)) Before and after laser annealing at a fluence of 100 mJ cm^{-2}.

of a fluence of 50 mJ cm^{-2}, the O1, O2, and O3 peaks shifted by 0.2, 0.03, and 0.2 eV, respectively, to higher energies, as compared with the case of as-grown nanowires. For the case of the laser energy density of 200 mJ cm^{-2}, the shift is more significant; the O1, O2, and O3 peaks shifted by 0.6, 0.5, and 0.5 eV, respectively, as compared with the case of as-grown nanowires.

The shift of Zn 2p and O 1s peaks towards higher binding energies after laser annealing can be explained by the increase of oxygen vacancies. The ionized oxygen vacancies acting as n-type dopants in ZnO materials donate two electrons to the conduction band. The increased electron density due to increased oxygen vacancies raises the Fermi level closer to the conduction band, but not into the conduction band [8]. The increased oxygen vacancies decrease the work function, and this is the reason why the O 1s peak shifts towards higher binding energies [8], as shown in figure 4(b). The integral intensity (i.e., area under the peak) ratio of O1/O2 increased with increasing fluence (figure 4(b)), which indicates that the O^{2-} bound ZnO(OH) species was reduced due to the recrystallization by laser annealing.

3.4. Electrical properties

The effect of laser annealing on the electrical properties of ZnO nanowires was also investigated. For this purpose, ZnO nanowires were fabricated into conventional nanowire FET device structures in a bottom-gate configuration, in which the gate electrode is located under the nanowires, as shown in figure 5(a). Figure 5(b) shows the FESEM image of a typical ZnO nanowires FET device with a single ZnO nanowire connected between source and drain electrodes.

Figure 5 shows representative data of the drain–source current versus drain voltage (I_{ds}–V_{ds}) curves measured at two different gate voltages and the drain–source current versus gate voltage (I_{ds}–V_g) curves measured at a fixed drain voltage of 1.0 V for ZnO nanowire FETs before and after laser annealing at fluences of 50 mJ cm^{-2} (figures 5(c) and (e)) and 100 mJ cm^{-2} (figures 5(d) and (f)). As-grown ZnO nanowires were transferred onto thermally-grown oxide on silicon substrates from the growth substrates. We measured the electrical characteristics of nanowire FETs on substrate (figure 5(b)). After laser annealing of these nanowire FETs, we measured again and compared their electrical properties. Note that nanowires are often broken into pieces after laser

Table 1. The electronic properties of ZnO nanowire FETs before and after laser annealing at fluences of 50 and 100 mJ cm^{-2}.

	Annealing at 50 mJ cm^{-2}		Annealing at 100 mJ cm^{-2}	
Device parameter	Before annealing	After annealing	Before annealing	After annealing
Threshold voltage (V)	11.3	− 0.7	6.2	− 9.9
Subthreshold slope (V/decade)	0.68	1.17	0.74	5.39
Carrier density (cm^{-3} at $V_g = 15$ V)	3.6×10^{17}	1.5×10^{18}	8.6×10^{17}	2.4×10^{18}
Mobility (cm^2 V^{-1} s^{-1})	16.6	12.3	16.3	27.9
I_{on}/I_{off}	$\sim 10^4$	$\sim 2 \times 10^4$	$\sim 2 \times 10^4$	$\sim 3 \times 10^2$

annealing at high fluences, as can be seen in the insets of figure 1. The data shown in figure 5 were measured for the nanowire FET devices that survived laser annealing. In the case of the fluence of 50 mJ cm^{-2}, five out of eight nanowire FET devices survived, and in the case of the fluence of 100 mJ cm^{-2}, two out of 12 nanowire FET devices survived.

After laser annealing, the drain current typically increased, and the threshold voltage (V_{th}) shifted in the negative gate bias direction. These phenomena can be explained by the generation of more oxygen vacancies which act as n-type dopants. The two as-grown ZnO nanowire transistors before laser annealing, shown in figures 5(c) and (d), were found to operate in a normally-off type, n-channel enhancement mode, which has off-current status at zero gate bias and a positive threshold voltage. After laser annealing, the ZnO nanowires transistors operated in a normally-on type, n-channel depletion mode, which exhibits nonzero current at zero gate bias and a negative threshold voltage. This threshold voltage shift in the negative gate bias direction after laser annealing is associated with the relative increase in the carrier density in laser-annealed ZnO nanowires. As summarized in table 1, the carrier density was calculated and compared before and after the laser annealing. The carrier density of laser-annealed ZnO nanowire transistors increased by a factor of 3–4 as compared with the case before laser annealing. As mentioned previously, the increase in the carrier density is due to the increase of oxygen vacancies (n-type dopants) by laser annealing. Note that some as-grown ZnO nanowire FETs exhibited depletion-mode device characteristics, i.e., $V_{th} < 0$. After laser annealing of these depletion-mode FETs, the threshold voltage V_{th} shifted more in the negative gate bias direction.

In addition to the carrier density, other electrical parameters, such as subthreshold slope and field effect mobility, were also determined and compared before and after laser annealing. In table 1, we summarize the threshold voltages, subthreshold slope, carrier densities, field effect mobility, and on/off-current ratio, which were extracted from figure 5. The field effect mobility (μ) of the nanowire FET can be calculated by [25, 26]

$$\mu = \frac{dI_{ds}}{dV_g}\frac{L^2}{V_{ds}C}, \tag{1}$$

where C is the gate capacitance given by equation (2) for a model of a cylinder on an infinite metal plate [25, 26],

$$C = \frac{2\pi\varepsilon_0\varepsilon L}{\cosh^{-1}(1 + t/r)}, \tag{2}$$

where r is the nanowire radius (50–100 nm), L is the nanowire channel length (~3 μm), t is the SiO_2 thickness (100 nm), ε_0 is the permittivity of free space, and ε is the dielectric constant of SiO_2 (3.9). The carrier density (n) can be calculated from $n = Q_{tot}/q\pi r^2 L$, in which total charge is $Q_{tot} = C|V_g - V_{th}|$. The carrier density was calculated at $V_g = 15$ V which was chosen arbitrarily because at this voltage the ZnO nanowires are in the on-current state for all of the cases (see figure 5).

The mobility values obtained from equation (1) were found to be similar within a factor of 2 before and after laser annealing. Particularly, in the case of the laser annealing at 100 mJ cm^{-2}, the off-current increased significantly due to the addition of more oxygen vacancies in the ZnO nanowires by the relatively high fluence, resulting in a reduced on/off ratio. The subthreshold swing values increased after laser annealing. The subthreshold swing (SS) is given by the inverse slope of the plots of the logarithm of the drain current versus gate voltage. The SS can be controlled by the ZnO doping level, as shown in the following equation (3), [27]

$$SS \equiv \frac{dV_g}{d\log I_{ds}} = 2.3\frac{kT}{q}\left(1 + \frac{1}{C}\sqrt{\frac{\varepsilon_0\varepsilon_{ZnO}qn}{\phi_s}}\right) \tag{3}$$

where ε_{ZnO} is the dielectric constant of ZnO, T is temperature, n is carrier density of ZnO nanowire, and ϕ_s is surface potential. The SS parameter of FETs for logic and memory applications describes how rapidly the switch turns on and off. The measured degradation of SS (i.e., increase of SS) after laser annealing thus directly corresponds to the increased carrier density caused by the generation of more oxygen vacancies after laser annealing, according to equation (3). The SS at higher fluence increased considerably, compared with that at lower fluence, because of the increase in oxygen vacancies in the ZnO nanowires.

4. Conclusions

We have demonstrated the effect of excimer laser annealing on the structural, optical, chemical bonding, and electrical properties of ZnO nanowires and their transistor devices. The

changes in nanowire morphology and photoluminescence after laser annealing are ascribed to the melting and rapid quenching of nanowires by high fluences. From XPS analysis of as-grown nanowires and laser-annealed nanowires, it can be concluded that oxygen vacancies act as n-type dopants and are increased by laser annealing. The threshold voltage of laser-annealed ZnO nanowire FET devices shifts in the negative gate bias direction owing to the increase in oxygen vacancies due to the laser annealing.

Acknowledgments

This work was supported through the National Research Laboratory (NRL) programme and the Proton Accelerator User Programme of Korea of the Korea Science and Engineering Foundation (KOSEF), the Programme for Integrated Molecular System at GIST, and the Basic Research Promotion Fund of the Korea Research Foundation Grant.

References

[1] Goldberger J, Hochbaum A I, Fan R and Yang P 2006 *Nano Lett.* **6** 973
[2] Huang Y, Duan X and Lieber C M 2005 *Small* **1** 142
[3] Yuan G-D, Zhang W-J, Jie J-S, Fan X, Tang J-X, Shafiq I, Ye Z-Z, Lee C-S and Lee S-T 2008 *Adv. Mater.* **20** 168
[4] Liao L *et al* 2008 *J. Appl. Phys.* **104** 076104
[5] Park W I, Yi G-C, Kim M and Pennycook S J 2003 *Adv. Mater.* **15** 526
[6] Wang Z L and Song J 2006 *Science* **312** 242
[7] Zhu R, Wang D, Xiang S, Zhou Z and Ye X 2008 *Nanotechnology* **19** 285712
[8] Remashan K, Hwang D-K, Park S-J and Jang J-H 2008 *Japan. J. Appl. Phys.* **47** 2848
[9] Oh M-S, Hwang D-K, Lim J-H, Choi Y-S and Park S-J 2007 *Appl. Phys. Lett.* **91** 042109
[10] Hatanaka Y, Niraula M, Nakamura A and Aoki T 2001 *Appl. Surf. Sci.* **175/176** 462
[11] Smith P M, Carey P G and Sigmon T W 1997 *Appl. Phys. Lett.* **70** 342
[12] Aoki T, Hatanaka Y and Look D C 2000 *Appl. Phys. Lett.* **76** 3257
[13] Zhao Y and Jiang Y 2008 *J. Appl. Phys.* **103** 114903
[14] Nagase T, Ooie T and Sakakibara J 1999 *Thin Solid Films* **357** 151
[15] Li M, Anderson W, Chokshi N, DeLeon R L and Tompa G 2006 *J. Appl. Phys.* **100** 053106
[16] Park S-H, Kim S-H and Han S-W 2007 *Nanotechnology* **18** 055608
[17] Chang P-C, Chien C-J, Stichtenoth D, Ronning C and Lu J G 2007 *Appl. Phys. Lett.* **90** 113101
[18] Hagemark K I 1976 *J. Solid State Chem.* **16** 293
[19] Lott K, Shinkarenko S, Kirsanova T, Türn L, Grebennik A and Vishnjakov A 2005 *Phys. Status Solidi* c **2** 1200
[20] Zhang S B, Wei S-H and Zunger A 2001 *Phys. Rev.* B **63** 075205
[21] Wang L and Giles N C 2003 *J. Appl. Phys.* **94** 973
[22] Zhang X T, Liu Y C, Zhi Z Z, Zhang J Y, Lu Y M, Shen D Z, Xu W, Fan X W and Kong X G 2002 *J. Lumin.* **99** 149
[23] Rosa E D L, Sepúlveda-Guzman S, Reeja-Jayan B, Torres A, Salas P, Elizondo N and Yacaman M J 2007 *J. Phys. Chem.* C **111** 8489
[24] Lu Y F, Ni H Q, Mai Z H and Ren Z M 2000 *J. Appl. Phys.* **88** 498
[25] Wang D, Chang Y-L, Wang Q, Gao J, Farmer D B, Gordon R G and Dai H 2004 *J. Am. Chem. Soc.* **126** 11602
[26] Maeng J, Jo G, Kwon S-S, Song S, Seo J, Kang S-J, Kim D-Y and Lee T 2008 *Appl. Phys. Lett.* **92** 233120
[27] Sze S M and Ng K K 2007 *Physics of Semiconductor Devices* (New Jersey: Wiley)